# Test observations at frequencies below 80 GHz at the IRAM 30m telescope

A. Belloche, S. Navarro, A. Sievers, C. Thum
J. Cernicharo, D. John, N. Marcelino, & K.M. Menten

July 28, 2004

**Abstract**

Both 3mm receivers, A100 and B100, can be made to work below 80 GHz in a special configuration AB* where they are pumped by the Gunns of the A230 and B230 receivers instead of their proper Gunns. In configuration AB* where then receivers A230 and B230 are not available, telescope and receiver optics worked correctly down to 68 GHz, the lowest frequency tested, and the telescope efficiencies are as expected. However, noise temperature and image gain $g_i$ are correct down to only $\sim$ 75 GHz, below which frequency both quantities tend to increase rapidly. The image gain is then observed to depend strongly on the tuning parameters and often varies considerably across the bandpass of the receiver. The Martin–Puplett based method for measuring the image gain has been extended to work on a channel by channel basis for the spectrometers, and it is strongly recommended that such image gain calibrations are made below 80 GHz. But even then calibration of the antenna temperature becomes difficult below 75 GHz, and observers are adviced to check the repeatability of the calibration and compare it against a known reference, like those provided with this report.

## 1 Background

The nominal frequency range of IRAM 3mm receivers is 80 – 115.5 GHz on the 30m telescope. Frequencies below 80 GHz were so far inaccessible, although the atmosphere is transparent until $\sim$ 66 GHz where absorption from atmospheric oxygen becomes prohibitively strong (zenith transmission 15% at the 30m site). Since several astrophysically important transitions are located in this so far inaccessible frequency range, we have conducted tests at the 30m telescope during 9–12 January and 18–22 May 2004 in order to explore to which degree the current 3mm receivers can be made to work below 80 GHz.

The nominal tuning range is limited by the range over which the local oscillator (a single Gunn) can be tuned. Outside the Gunn tuning range, mixer and waveguide properties, and the feed/lens optics must be expected to deteriorate. The main goal of the tests was to determine how serious these deteriorations are and where exactly they set in. We also wanted to get an idea how the special setup employed for observations outside the nominal tuning range affects the receiver operation and, by consequence, the practical feasibility of such observations.

## 2 Setup

To overcome the limitation due to the 3mm local oscillator (LO), we used the LO of the A230 and B230 receivers whose Gunn can be tuned from 65.5 to 89 GHz. Two pieces of semirigid waveguide were used to transport the LO signals from A230 and B230 to the A100 and B100 LO boxes.

The synthesizer control software had to be modified for the tests in order to obtain a correct Doppler tracking of A100 and B100. If frequencies below 100 GHz are sent to the A230 and B230 receivers, the modified software recognizes that these frequencies are meant for the A100 and B100 receivers. It resets the frequency limits appropriately and switches off the frequency multiplication. The modification is fully transparent to the user and worked correctly.

The use of the A230 and B230 LO for the A100 and B100 receivers naturally excludes that A230 and B230 can be used for observations. Most test observations in May 2004 were therefore done using only A100 and B100 in parallel. This unfortunate loss of A230 and B230 could in theory be overcome if the LO signals from the C or D receivers were used to pump A100 and B100. Apart from the need for longer cables (not available) the LO signals may have to be amplified and major modifications of the synthesizer hardware (and software) are needed.

The test observations below 80 GHz done in January 2004 were made only with the B100 receiver. Therefore we used the B100 in parallel with A100 and A230, i.e. in a truncated AB configuration. Tests in May 2004 were made with both 3mm receivers modified for < 80 GHz.

# 3 Scope of tests made

## 3.1 Frequencies tuned

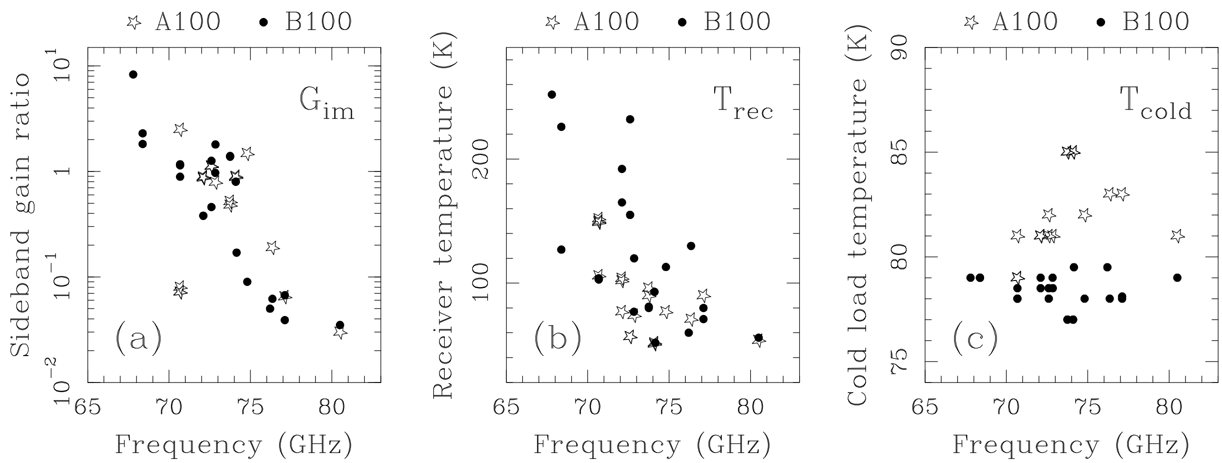


Figure 1: Continuum sideband gain ratio **(a)**, receiver temperature **(b)**, and cold load temperature of the A100 and B100 **(c)** for all frequencies tuned below 80.5 GHz.

The characteristics of the A100 and B100 receivers at all the frequencies tuned below 80.5 GHz during the tests are shown in Fig. 1. The general trend for both receivers is an increase of the receiver temperature and the sideband gain ratio when the frequency decreases (Fig. 1 a and b). In most cases above 70 GHz, *a tuning with a receiver temperature (measured with VESPA) below ~ 120 K could be found for both receivers.* Below 70 GHz, the receiver temperatures were larger than 150-200 K. The receiver temperatures were not significantly different when measured with VESPA or the continuum backend. The mean differences and standard deviation $T_{\rm rec}^{\rm vespa} - T_{\rm rec}^{\rm cont}$ are $2 \pm 7$ K and $1 \pm 15$ K for the two receivers.

*Good sideband gain ratios below 0.1 were obtained above 75 GHz* (see Fig. 1a). However, the sideband gain ratio approached 1 (DSB) below 75 GHz, and was even larger (USB) at the smallest tuned frequency (8.3 at 67.8 GHz). However a good sideband gain ratio of 0.07 was obtained for A100 at 70.68 GHz with a receiver temperature of 160 K. This suggests that tunings with sideband gain ratios smaller than 0.1 can still be found in the range, at least at 70-75 GHz, provided that more time is spent trying several positions of the mixer backshort (see Appendix B).

The carbon star IRC+10216 was observed at several frequencies between 70 and 80 GHz. All the lines detected with both receivers have the same velocity width. We conclude that both receivers are not sensitive to mixing products with the second LO harmonic ($2 \times \nu_{\rm LO} \pm \nu_{\rm IF}$).

## 3.2 Frequency switching

We tested the Frequency Switch observing mode below 80 GHz during the May session. During the tests, the hardware did not handle properly the frequency throws set by the observer. While the headers of the A100 and B100 spectra contained the frequency throws set by the observer to A100 and B100 with the command FSWITCH in OBS, the actual values measured in the spectra were equal to one third of the throws set to A230 and B230, whose local oscillators were used to tuned A100 and B100 below 80 GHz. The reason is that, for the A230 and B230 receivers used at usual frequencies, the frequency throws given by the observer are first divided by 3 to tune the Gunn and then remultiplied by 3 after the Gunn. Therefore, with the current hardware setup, the observer has to set the frequency throws of A230 and B230 to 3 times the throws desired for A100 and B100. The frequency throws contained in the headers

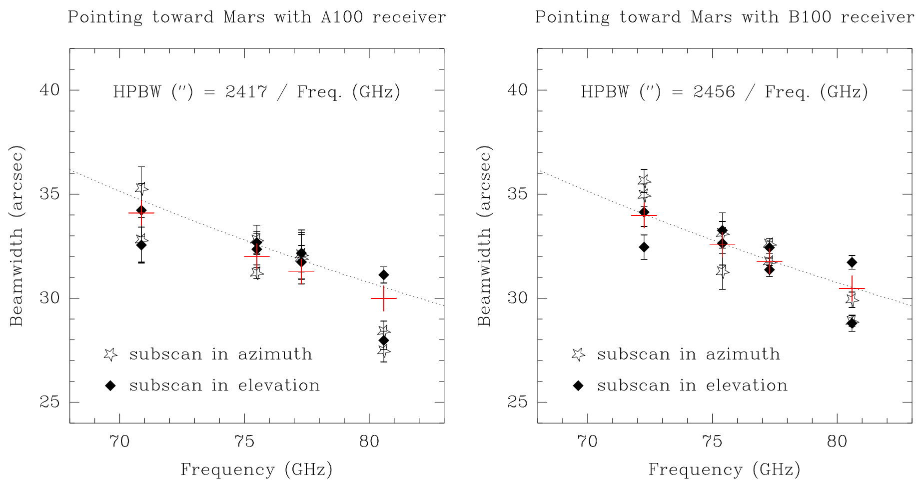


Figure 2: Pointings on Mars with the A100 (*left*) and B100 (*right*) receivers. The beam width (FWHP) is plotted versus frequency. For each receiver, the red crosses show the best fit model to the data, and the fit result is written at the top of the panel. Symbols are plotted at their effective, i.e. sideband–weighted, frequency, and the beam widths are deconvolved (Mars diameter 4.1"). In each panel, the dotted curve shows the extrapolation of the canonical relation observed for frequencies above 80 GHz.

of the A100 and B100 spectra and the actual frequency throws will then match each other. However, another solution is to remove in the hardware setup this division/multiplication when the A230 and B230 LO are used to tune A100 and B100 below 80 GHz.

It is aimed that frequency switching will work correctly when the first scheduled < 80 GHz observations will be made, but at the moment of writing this report it is not clear whether this goal will be reached.

## 3.3 Beam

The beam size at frequencies $\nu < 80.5$ GHz was measured toward a few pointing sources (Fig. 2). The best fit models shown in this figure for A100 and B100 are

$$\mathrm{HPBW}('') = 2417/\nu(\mathrm{GHz}) \qquad \mathrm{(A100)}$$

$$\mathrm{HPBW}('') = 2456/\nu(\mathrm{GHz}) \qquad \mathrm{(B100)}$$

with rms residuals of 1.2" and 1.0", respectively. This is in good agreement (better than 2%) with the canonical relation HPBW(") = 2460/$\nu$(GHz) obtained at higher frequencies (see IRAM Newsletter 58). We conclude from these results that the lens/feed optics work correctly down to at least 68 GHz.

## 3.4 Focus

In Fig. 3, we show the difference of the axial focus position `SFCZ` between the two receivers A100 and B100, for both sets of observations (January and May 2004). In January, when only B100 was tuned below 80 GHz, we find a small (−0.3 mm), but hardly significant difference, possibly suggesting that SFCZ may be slightly increasing with frequency near 80 GHz.

In May, most of the time both receivers were tuned below 80.5 GHz to the same frequency No systematic focus difference was noticed between both receivers albeit with considerable measurement uncertainty. The rms dispersion is ~0.5 mm, probably dominated by measurement error during the often unstable conditions during the May test.

## 3.5 Aperture and beam efficiencies

Using pointings toward 6 planets and *assuming* a forward efficiency $F_{eff} = 0.95$, the mean ratio of flux density to antenna temperature is $5.9 \pm 0.3$ Jy K$^{-1}$ for A100 and $5.7 \pm 0.1$ Jy K$^{-1}$ for B100, after correction for the finite size of each source (see Fig. 4). This yields a mean aperture efficiency $\eta_a = 0.63 \pm 0.03$ for A100 and $\eta_a = 0.65 \pm 0.02$ for B100 in the frequency range 70-80 GHz. These two

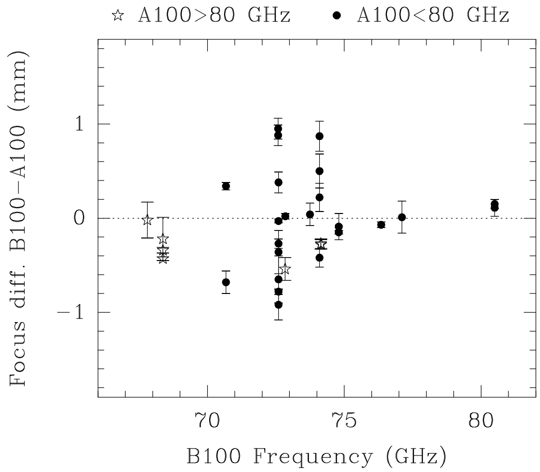


Figure 3: Focus difference between the A100 and B100 receivers, when B100 was tuned below 80.5 GHz but A100 was always tuned at 93.176 GHz in January (*star symbols*) and when both receivers were tuned below 80.5 GHz at the same frequency in May (*black dots*).

values are compatible with the aperture efficiency of 0.64 expected at 75 GHz from a linear extrapolation of the aperture efficiencies measured in the frequency range 86-279 GHz (see the IRAM Newsletter 58). Assuming a Gaussian beam with HPBW(") = $2440/\nu$(GHz), the beam efficiencies derived from these aperture efficiencies are $B_{eff} = 0.79 \pm 0.04$ for A100 and $B_{eff} = 0.81 \pm 0.02$ for B100 at 75 GHz.

# 4 Results

In Tab. 1, we summarize the results of the spectroscopic observations made in January and May. The transitions were selected with the aim of covering the frequency range of 66 – 80 GHz and of finding tuning parameters for some of the important lines. Numerous lines were detected which allowed cross checking of the antenna temperature calibration scale with existing information. This process is not yet complete.

The table shows that the image gain factor $g_i$ systematically increases with decreasing $\nu$, a trend which is already obvious from Fig. 1. Below $\sim$74 GHz, the power in the image band is $\gtrsim 0.2$ and thus not negligible anymore. $g_i$ has to be measured precisely in order to avoid calibration errors. At about the same frequency the tuning behavior becomes erratic. At a few frequencies where several mixer backshort peaks were tried, sometimes very different $g_i$ and $T_{rec}$ were obtained. In the range 70 –74 GHz, care must therefore be taken to obtain the optimum tuning and a precise measurement of $g_i$ (see below) is mandatory.

Below 70 GHz where both $g_i$ and the receiver temperature are high, no lines are detected anymore. We conclude that both A100 and B100 are then beyond their useful frequency range.

As an example that it makes sense to use the 30m telescope below 80 GHz even with the described limitations of its present 3mm receivers, we show in Fig. 5 the rotational ground transition at 77.1 GHz of $N_2D^+$ toward the dense dark core of B1 (position from Gerin et al. 2001), accompanied by the corresponding transition of $N_2H^+$ at 93.2 GHz. A representative sample of test spectra, covering the range of 80 - 72 GHz, is available at URL[1] `./IRAMFR/PV/lowfreqs/spectra.html`.

These spectra are shown as calibrated by the standard RED calibration as long as the bandpass–averaged (i.e. measured with a continuum backend) image gain factor $g_i \lesssim 0.2$. Above this threshold noticable calibration errors must be expected, if $g_i$ is not flat across the backend bandpass. The exact channel–to–channel image gain factor $g_i(\nu)$ should then be measured (Appendix A) and calibrated in OTFCAL (Appendix B).

a small manual on how to compute the sideband gain ratios for spectral line backends. You can find this manual in the directory /mrt-lx1/vis/default/cal/ as calssb.pdf or calssb.ps The OTFCAL procedures inissb.cal and ssb.cal can also be found in the same directory.

In a shortcut which is for our test purposes sufficiently accurate, we multiplied the RED–calibrated

[1]The leading dot substitutes for `http://www.iram.fr` or its mirror `http://www.iram.es`

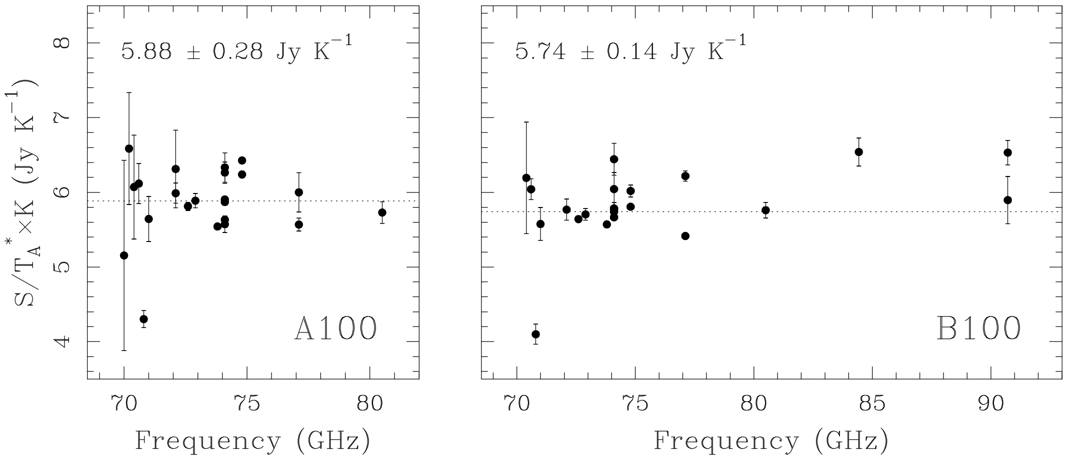


Figure 4: Ratio of the flux density $S_\nu$ over the antenna temperature $T_A^\star$ observed toward planets with the A100 (*left*) and B100 (*right*) receivers. Each ratio was multiplied by $K = (1 - \exp(-x^2))/x^2$ with $x^2 = \ln 2 \times D/\mathrm{HPBW}$ to account for the finite diameter $D$ of each source (see Kramer 1997). We used HPBW(") = $2440/\nu$(GHz), a forward efficiency $F_{eff} = 0.95$ and a flux density $S\nu$ corrected for the sideband gain ratio $G_{im}$: $S = (S_{lsb} + G_{im} S_{usb})/(1 + G_{im})$. The mean ratio is written in the top left corner of each panel and is plotted as a dotted line. The extreme low point at 70.7 GHz was left out of the fit for both receivers. For the clarity of the figure, the many measurements made at 70.7 GHz are spaced out between 70 and 71 GHz.

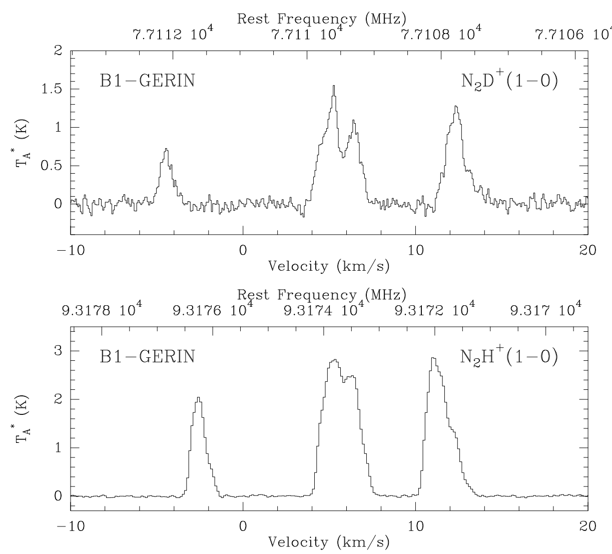


Figure 5: $N_2H^+$(1-0) and $N_2D^+$(1-0) spectra obtained toward the dense core B1.

spectra by the correction factor

$$(1 + G^{\mathrm{l}}_{\mathrm{im}}(\nu))/(1 + G^{\mathrm{c}}_{\mathrm{im}})$$

# 5 Conclusions

The frequency range below 80 GHz, the current lower end of the 3mm tuning range, down to 66 GHz where strong absorption by the atmospheric $O_2$ sets in was investigated by pumping the 3mm receivers A100 and B100 with the Gunn signals from A230 and B230 respectively. We show that the telescope and receiver optics behave correctly down to 68 GHz, and the telescope efficiencies have the expected values. Below this frequency, no measurements were made, because of the rapidly increasing receiver temperature.

Table 1: Results obtained in January (J) and May (M) with the A100 or B100 receiver with a bandwidth of 500 MHz centered at the frequencies tuned below 81 GHz.

| Frequency (GHz) | Line | Date | $G_{im}$ | Source | Lines detected |
|---|---|---|---|---|---|
| 80.5 | HDO | J | 0.031 | W51e1/e2 | standard Rxs, various lines |
| | | J | 0.031 | IRc2 | compare/standard Rxs, various lines |
| | | M | 0.03 | W3(H2O) | HDO detected at 0.055 K |
| 77.1 | $N_2D^+$ | J | 0.039 | L1448 | detected at 0.4 K |
| | | J | | B1 | detected at 1.5 K |
| | | M | 0.067 | B1 | detected at 1.5 K |
| 76.4 | $DOC^+$ | M | 0.062 | K3-50 | no lines detected ($<$ 0.02 K) |
| | | M | | W51E1E2 | many lines up to 1.3 K |
| 76.2 | l–$C_3H$ | J | 0.05 | B1 | no $C_3H$, but DNC (3K), $C_4H$ |
| | | J | 0.05 | TMC 1 | no $C_3H$, but DNC (0.5K), $C_4H$ |
| 74.8 | H44$\alpha$ | M | 0.09 | K3-50A | H44$\alpha$ 0.55 K, He44$\alpha$ 0.07 K, H55$\beta$ 0.2 K |
| | | M | | W51DW5 | H44$\alpha$ 1.0 K, He44$\alpha$ 0.1 K, H55$\beta$ 0.3 K |
| 74.2 | $CH_3OCH_3$ | J | 0.17 | DR21(OH) | detected at 0.05 K ? (3$\sigma$) |
| | | J | 0.17 | B1 | $N_2D^+$ from USB |
| 74.1 | $HCNH^+$ | M | 0.80 | W51E1E2 | many lines, up to 0.3 K |
| | | M | | IRC+10216 | main line (0.7 K) USB |
| 72.9 | $H_2CO$ | M | $\sim 1$ | IRC+10216 | 2 LSB lines, 3 and 1 K |
| 72.8 | $H_2CO$ | J | 0.97 | G75.78 | line 1.5 K, other lines |
| | | J | | 20126+4104 | line 1.0 K, other lines |
| | | J | | DR21(OH) | line 3.0 K, other lines |
| | | J | | Cep A | line 1.5 K, other lines |
| 72.6 | $H_2CO$ | J | 1.84 | IRc2 | many lines |
| | | J | 1.17 | G75.78 | $H_2CO$ detected at 0.7 K |
| | | J | | MWC39 | line $<$ 0.1 K |
| | | M | $\sim 1$ | ORI-KL | $H_2CO(1_{01}\text{-}0_{00})$ 7-9 K, -$(5_{14}\text{-}5_{15})$ 4 K, DCN 1 K |
| 72.1 | $DCO^+$ | M | 0.38 | L183 | detected at 2.5 K |
| 70.7 | $CH_2$ | M | 0.072 | W51-M | detected at 0.05 K ? |
| | | M | | ORI-KL | not detected |
| | | M | | IRC+10216 | $SiC_2$ 0.35 K, $H^{13}CCCN$ 0.15 K |
| 68.4 | $CH_2$ | J | 1.82 | IRc2 | line $<$ 1 K |
| | | J | | CRL618 | line $<$ 1 K |
| | | J | | | line $<$ 0.5 K |
| | | J | $\sim 2.3$ | B1 | line $<$ 0.5 K, noise not uniform |
| | | J | | L1448 | line $<$ 0.5 K, noise not uniform |
| | | J | | IRc2 | line $<$ 0.5 K, noise not uniform |
| 67.8 | $H_2O$ | J | 8.3 | IRc2 | manual cal., line $<$ 2 K |
| | | J | 8.3 | NML Tau | manual cal., line $<$ 2 K |

In the range of 77 – 80 GHz the receiver temperature and image gain have values indistinguishable from those at $\gtrsim 80$ GHz, and both receivers can be used correctly. Below 77 GHz, the image gain $g_i$ starts to increase and reaches a value of $\sim 0.2$ near 74 GHz. Below 72 GHz the receivers become DSB or essentially USB. Furthermore, the tuning behavior becomes erratic, sometimes being very different between peaks of the mixer backshorts at the same frequency. We also found that $g_i$ varies strongly across the receiver bandpass.

Accurate calibration of the antenna temperature becomes then very difficult, and we recommend that the 3mm receivers should not be used below 72 GHz. In the range 72 – 77 GHz where $g_i$ could be 0.2 or higher, we strongly recommend to measure for each tuning the channel–to–channel values of $g_i(\nu)$ with the Martin–Puplett based method described in the appendices.

Access to the extended tuning range below 80 GHz currently comes at a considerable price: *(i)* the 1.3mm receivers cannot be used simultaneously as usual in the configuration AB, *(ii)* the tuning range of the 3mm receivers has upper limits of 92.5 (A100) and 94.2 (B100), and *(iii)* most importantly, the "low frequency LO" has to be connected in a non–trivial manual operation, and $< 80$ GHz observations are therefore practical only during predetermined periods.

These problems may partially be overcome in the near future after the installation of special waveguide switches. These switches will swap the LOs between 3 and 1.3mm receivers A and B. In the special ("swapped") receiver configuration AB$^*$, the tuning ranges of the 3mm receivers will however still be limited as in *(ii)*, and furthermore the 1.3mm receivers cannot be tuned below 241 GHz.

More complete, but more difficult and expensive solutions are conceivable, like e.g. using the LOs of the C or D receivers for pumping the 3mm Rxs. We recommend however that the demand on $<$80 GHz time is monitored for some time before any further steps are considered.

# Appendix A: Measurement of the sideband gain ratio

The sideband gain ratio $G_{im} = \frac{G_i}{G_s}$ at the 30m telescope can be measured with the calibration procedure "cal /ssb REC"(with REC the name of the receiver) in the observing software OBS. This procedure consists of 4 subscans. The Martin Pupplet interferometer is first moved to select the lower sideband. The hot load and cold load are successively put in front of the receiver and the counts $C_l^h$ and $C_l^c$ are recorded. The same measurements $C_u^h$ and $C_u^c$ are done for the upper sideband. The gain ratio of the two sidebands is computed with the following equation:

$$G_{im} = \frac{C_u^h - C_u^c}{C_l^h - C_l^c} \tag{1}$$

This procedure yields the mean sideband gain ratio $G_{im}^c$ in the bandpass if the continuum backend is connected or the sideband gain ratio $G_{im}^l(\nu)$ as a function of frequency $\nu$ in the bandpass if a line backend is connected.

The spectra are calibrated with a uniform gain which is usely set as $G_{im}^c$ by the observer. However, the sideband gain ratio is not uniform in the bandpass of the receiver. This is a problem at frequencies below 80 GHz since the sideband gain ratio can reach values close to or even larger than 1. In that case, it is crucially needed to recalibrate the spectra with the true sideband gain ratio $G_{im}^l(\nu)$ (see Appendix B).

When using the A100 and/or the B100 receivers below 80 GHz, the observer can follow this procedure in OBS to measure the sideband gain ratio:

| | |
|---|---|
| continuum broad switching /rec A100 | ! Select the continuum backend. |
| cal /ssb A100 | ! Measure $G_{im}^c$ for the A100 receiver. The |
| | ! result is printed on the blue OBS window and |
| | ! should be read on the fly by the observer. |
| set gain $G_{im}^c$ /rec A100 | ! Set the image gain ratio to $G_{im}^c$. |
| vespa ... /rec A100 | ! Select the line backend. |
| cal /ssb A100 | ! Measure $G_{im}^l(\nu)$. The observer will have to |
| | ! compute this gain in OTFCAL with the |
| | ! procedure ssb.cal which reads the results of the 4 |
| | ! subscans in the raw data file. It produces an array |
| | ! containing $G_{im}^l(\nu)$ which can be written |
| | ! like a spectrum in a data file gain.30m. |

Note that the operator has to reset the Martin Pupplet after the use of the cal /ssb procedure. If it is not done, the receiver temperature will be anomalously high.

# Appendix B: Non-uniformity of the sideband gain ratio

The sideband gain ratio was measured following the procedure described in Appendix A. It was very sensitive to the position of the mixer backshort used for the tuning. We show in Fig. 6 the case of two tunings done at 70.7 GHz. In both cases, the sideband gain ratio was highly non-uniform. The tuning was double sideband in the first case but lower sideband in the second case, with a higher receiver temperature however. This example shows that a good sideband rejection may be found at least down to 70.7 GHz, provided that enough positions of the mixer backshort are tried.

For frequencies below 75 GHz, the continuum sideband gain ratio was often approaching 1, so that a recalibration of the spectra was needed to account for the non-uniformity of the sideband gain ratio in the bandpass. As a zero-order correction, we multiplied the spectra by the factor $(1+G_{\rm im}^{\rm l}(\nu))/(1+G_{\rm im}^{\rm c})$, following equation (6) of Kramer (1997).

As an example, we show in Fig. 7 the spectra obtained toward ORI-KL, before (black) and after (red) correction for the non-uniform sideband gain ratio (the red spectra were slightly shifted along the velocity axis to improve the clarity of the figure). The curves in blue represent the sideband gain ratios $\mathrm{G}_{im}^l(\nu)$. Before correction, A100 (calibrated with $\mathrm{G}_{im}^c = 1.12$) had stronger lines at low frequency and weaker lines at high frequency than B100 (calibrated with $\mathrm{G}_{im}^c = 1.26$). After correction, the lines match within 25%. Note that the 5$^{\rm th}$ line at $\sim$ -325 km s$^{-1}$ is the superposition of a LSB line and a USB line (identified by changing the LSR velocity). All the other lines are LSB.

It should be possible to obtain a calibration accuracy better than 25% by recalibrating the raw data

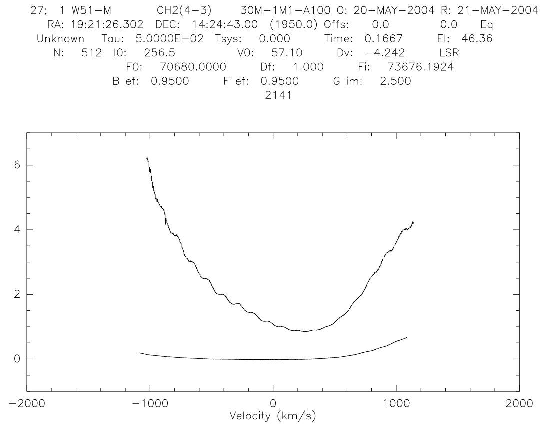

Figure 6: Sideband gain ratio of the A100 receiver centered at 70.7 GHz measured for two different positions of the mixer backshort. The first position (*upper curve*) gave a mean sideband gain ratio of 2.5 and a receiver temperature of $\sim$ 110 K with the continuum backend. For the second position (*lower curve*), they were 0.072 and $\sim$ 150 K, respectively.

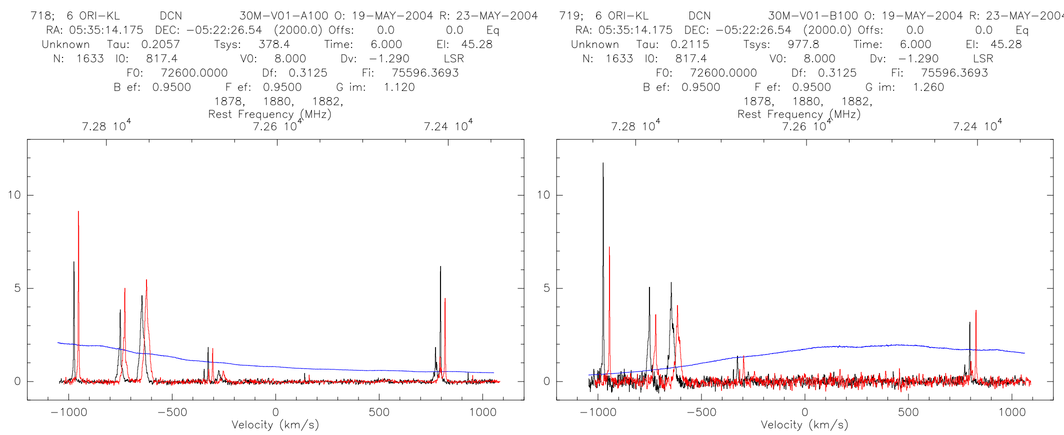

Figure 7: Spectra obtained at 72.6 GHz toward ORI-KL with the A100 (*left*) and B100 (*right*) receivers. The initial spectra are shown in black and the recalibrated spectra, slightly shifted along the velocity axis for clarity, are shown in red. The curves in blue represent the sideband gain ratios $G^l_{im}(\nu)$ measured with the procedure cal /ssb in OBS and computed with the procedure ssb.cal in OTFCAL.

and using a channel-dependent calibration factor $T_{cal}$ (see Eq. (6) of Kramer 1997). The atmospheric opacity derived from the atmospheric model should be computed for each channel using the spectral sideband gain ratio $G^l_{im}(\nu)$ instead of the uniform gain set by the observer in OBS (usually, $G^c_{im}$). The sky temperature $T_A^{sky}$ should also be measured for each channel.

Albrecht Sievers has written a small manual on how to compute the sideband gain ratios for spectral line backends. You can find this manual in the directory `/mrt-lx1/vis/default/cal/` as calssb.pdf or as calssb.ps. The OTFCAL procedures inissb.cal and ssb.cal can also be found in the same directory.

# References

Kramer, C. 1997, "Calibration of spectral line data at the IRAM 30m radio telescope", Version 2.1, IRAM Report (see http://www.iram.fr)

Gerin et al. 2001, ApJ 551, L193